THE PUBLISHING HOUSE
OF THE ROMANIAN ACADEMY

*PROCEEDINGS OF THE ROMANIAN ACADEMY, Series A,*
*Special Issue/2018, pp. 154–159*

# ANALYSIS OF THE THERMAL PERFORMANCE OF SINGLE AND MULTI-LAYERED MICROCHANNELS WITH FIXED VOLUME CONSTRAINT

OLAYINKA O. ADEWUMI[1], TUNDE BELLO-OCHENDE[2], JOSUA P. MEYER[1]

[1] University of Pretoria, Department of Mechanical and Aeronautical Engineering, South Africa
[2] University of Cape Town, Department of Mechanical Engineering, South Africa
Corresponding author: Olayinka O. ADEWUMI, E-mail: u12217400@tuks.co.za

**Abstract.** This study presents a numerical analysis of forced convection heat transfer and steady, laminar, incompressible fluid flow through single-, two- and three-layered microchannels with different flow arrangements and fixed total volume constraint. Previous studies on multi-layered microchannel heat sinks have shown that these types of heat sinks perform better than single-layered microchannel in terms of reducing thermal resistance and pressure drop, but this is obtained with increased total volume of the solid substrate because equal volumes of the single-layered microchannel are stacked to obtain the number of desired layers. In this paper, the total volume of the solid substrate for all the microchannels considered was fixed at 0.9 mm$^3$ and the geometries of the different microchannels were optimised based on the objective of maximising the thermal conductance using a computational fluid dynamics package with a goal-driven optimisation tool. The results show that for a fixed total volume and fixed inlet fluid velocity, the pumping power of the two-layered microchannel with the different flow arrangements was 10% less than that required for the single-layered microchannel but was increased by about 12% when the number of layers was increased to three. The results obtained from this study show that the multi-layered microchannels give very good results without increasing the total volume of the solid substrate as presented in previous investigations.

***Key words*:** Forced convection, Maximised thermal conductance, Pumping power, Pressure drop, Temperature rise, Fluid velocity.

## 1. INTRODUCTION

In recent times, stacked microchannel heat sinks, which integrate many layers of microchannels, have been developed to provide efficient thermal management at relatively low pressures while maintaining uniform chip temperature [1–4]. The design of stacked microchannel heat sinks found in literature provide larger flow passages with the aim of reducing pressure drop significantly for a constant heat flux. The larger flow passages are a result of the increase in total volume, as equal volumes of single-layered microchannels are stacked to achieve the desired number of layers. The multi-layered microchannel heat sink geometries in the outlined studies had increased total volume ($\geq 100\%$) more than the single-layered microchannel because the total volume of the solid substrate had to be doubled, tripled and so on, depending on the number of layers in the stack. With microelectronics devices becoming smaller, increasing the volume of the solid substrate is a disadvantage because of space constraints in these devices. Aside from the increase in volume, there is also increase in weight which is often discouraged in recent electronic device designs. This is why it is crucial to investigate how the multi-layered microchannel performs under a volume constraint. The optimisation of the multi-layered microchannel heat sink will be based on minimising the peak temperature of the solid substrate, which results in maximising the thermal conductance of the highly conductive silicon substrate [5]. Comparison between the pumping power and pressure drops for the different microchannels is also investigated.

## 2. MODEL DESCRIPTION AND MATHEMATICAL FORMULATION

Figure 1 shows the elemental volume used as computational domain for the single-, two- and three-layered microchannel while Fig. 2 shows the different flow configurations considered in this study.

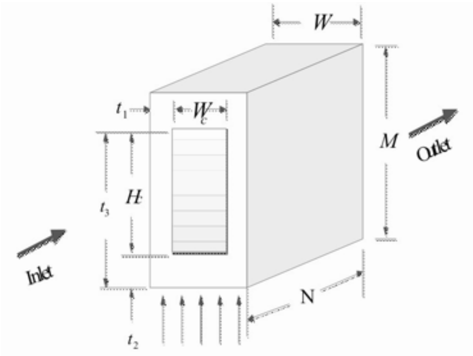


a)

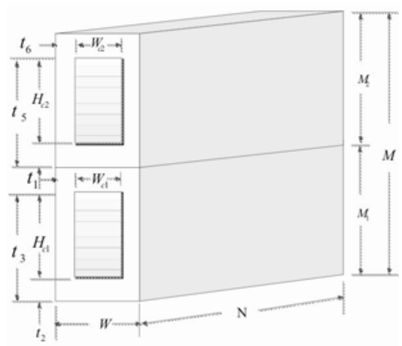

b)

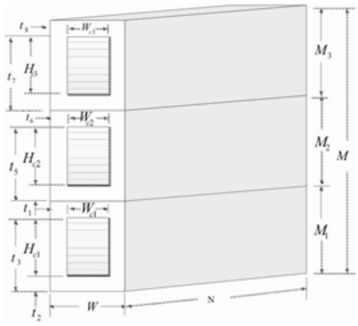

c)

Fig. 1 – Similarity temperature profiles: a) present study; b) comparison between present study and Kuiken.

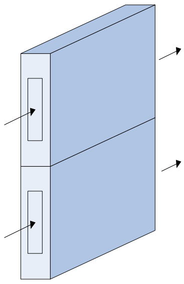

Parallel flow (PF)

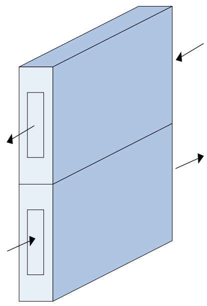

Counter-flow (CF)

a)

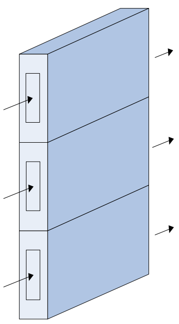

Parallel flow (PF)

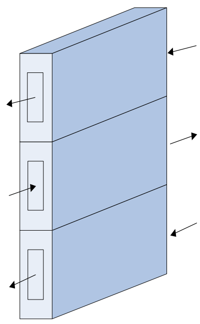

Counter-flow1 (CF1)

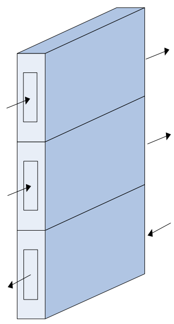

Counter-flow2 (CF2)

b)

Fig. 2 – Flow configurations for microchannel heat sink: a) two-layered stack; b) three-layered stack.

The heat transfer in the elemental volume is a conjugate problem that combines heat conduction in the solid and convective heat transfer in the liquid. The pressure difference drives the working fluid through the microchannels as a result of pumping power that is applied at the channel inlet. The flow and heat transfer are assumed to in steady-state conditions, incompressible flow, constant thermophysical properties with negligible radiation heat transfer.

### 2.1. Governing equations, boundary conditions and numerical procedure

The continuity, momentum and energy equations (equations 1 to 4) along with the specified boundary conditions were solved numerically using ANSYS Fluent computational fluid dynamic package, which employs a finite volume method. The solution is assumed to converge when the normalised residuals of the continuity and momentum equation fall below $10^{-5}$, while that of the energy equation falls below $10^{-7}$

$$\nabla \cdot \mathbf{v} = 0\,, \tag{1}$$

$$\rho \mathbf{v} \nabla \cdot \mathbf{v} = -\nabla p + \mu \nabla^2 \mathbf{v}\,, \tag{2}$$

$$\rho_f C_{p,f} \mathbf{v} \cdot \nabla T = k_f \nabla^2 T\,, \tag{3}$$

$$k_s \nabla^2 T = 0\,. \tag{4}$$

The heat flux between the interface of the fluid and the solid walls is coupled and its continuity between the interface of the solid and the liquid and the dimensionless global thermal conductance, which is the measure of performance is stated in equation (5). Equation (6) shows the expressions for the temperature rise on the heated wall and pumping power respectively. The flow boundary conditions are: no slip and no penetration at the wall surfaces, $u = u_{\text{in}}$, $v = w = 0$ m/s at the inlet and zero stress at the outlet. The thermal boundary conditions are specified as $T = T_{\text{in}}$ at the inlet, while symmetry boundary conditions are specified at the left and right side of the computational domain. A constant uniform heat flux $q''$ is applied at the bottom wall, while no heat flux is applied at the top wall.

$$k_s \left.\frac{\partial T}{\partial n}\right|_{\Omega} = -k_f \left.\frac{\partial T}{\partial n}\right|_{\Omega} k_s \left.\frac{\partial T}{\partial n}\right|_{\Omega} = -k_f \left.\frac{\partial T}{\partial n}\right|_{\Omega}\,,\quad C = q'' N k_f \Delta T\,,\quad \Delta T = T_{\max} - T_{\min}\ \ \Delta T = T_{\max} - T_{\min}\,, \tag{5}$$

$$\Delta T_{base} = T_{\max} - T_{\min,\,base}\,, \tag{6}$$

$$P_P = u_{in} A_c \Delta P\ \ P_P = u_{in} A_c \Delta P\,. \tag{7}$$

### 2.2. Numerical optimization procedure

The length $N$, height $M$ and width $W$ of the solid is fixed, which makes the total volume of the single-, two- and three-layered microchannel $V$ fixed as shown in equation (8), while $t_1$, $t_2$, $t_3$, $t_5$, $t_6$, $t_7$, $t_8$, $H_c$, $H_{c1}$, $H_{c2}$, $H_{c3}$, $W_c$, $W_{c1}$, $W_{c2}$ and $W_{c3}$ are varied, but also subject to manufacturing constraints shown in equations (9) to (11).

$$V = MWN = \text{const.}, \tag{8}$$

$$H_{c1\text{-}c3}/W_{c1\text{-}c3} \le 20,\ t_2 \ge 50\ \mu\text{m}, \tag{9}$$

$$M - t_3 \ge 50\ \mu\text{m},\ M_2 - t_5 \ge 50\ \mu\text{m},\ M_3 - t_7 \ge 50\ \mu\text{m}, \tag{10}$$

$$M_1 + M_2 + \ldots + M_n = M\,. \tag{11}$$

Goal driven optimisation tool (GDO) is an optimisation technique that finds design candidates from the response surfaces. The accuracy of the response surface for the design candidates is checked by converting it to a design point and, thereafter, a full simulation is carried out for that point to check the validity of the output parameters. Numerical simulations and optimisation were carried out for a fixed total volume $V$ of 0.9 mm$^3$

with fixed axial length $N$ of 10 mm, total height $M$ of 900 μm and width $W$ of 100 μm. The temperature of water pumped across the microchannel was 20°C and heat flux applied to the bottom wall was $10^6$ W/m$^2$. The design space for the response surface for the fixed total volume was defined as $54 \leq W_{c1}, W_{c2}, W_{c3} \leq 66$ μm, $50 \leq M - t_3 \leq 60$ μm, 25 μm $\leq M_1 - t_3, M_2 – t_5 \leq 30$ μm and 240 μm $\leq H_{c1}, H_{c2}, H_{c3} \leq 375$ μm. The optimised design point chosen was required to meet the manufacturing constraints.

## 3. RESULTS AND DISCUSSION

The results obtained for the two- and three-layered microchannel heat sinks in the present study were compared with those obtained for the single-layered microchannel in our previous study [5]. The corresponding inlet fluid velocity was between 0.329 m/s to 1.865 m/s for pressure drop of 10 kPa to 60 kPa considered. The range of Reynolds number ($Re_{Dh}$) for these velocities is $36 < Re_{Dh} < 210$. Therefore, in this study, the inlet velocity of fluid flow into each channel of the two- and three-layered microchannels were exactly the same as those of the single-layered microchannel.

### 3.1. Comparison between maximised thermal conductance of single and multi-layered microchannels with the same total volume

Figure 3 shows the comparison between the maximised thermal conductance of the single and multi-layered microchannels with different flow arrangements. Results obtained show that for the same total volume of solid substrate, increasing the microchannel layers to three improves the thermal performance of the microchannel for inlet velocities greater than 0.648 m/s.

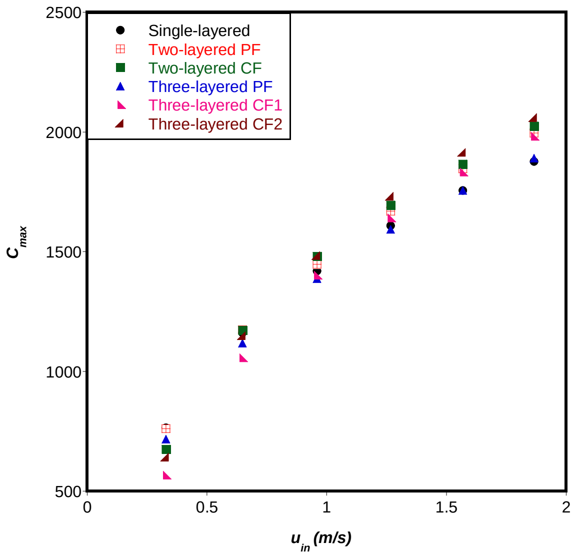


Fig. 3 – Comparison between the maximised thermal conductance of the single-, two- and three-layered microchannels at different velocities.

### 3.2. Comparison between pumping power in single- and multi-layered microchannel with the same total volume

Figure 4 shows the comparison between the pumping power requirements for the different fluid inlet velocities in the single- and two-layered microchannels. It was observed that, as the velocity of the fluid increased, the required pumping power increased, which is the expected trend. However, the results presented in Fig. 4a show that the bottom channel required 40% to 50% more pumping power for fluid flow than the top channel. This was because the bottom channel is in direct contact with the heated base. Consequently, more cooling was needed at the bottom layer than at the top layer. Figure 4b shows that the total pumping power required for the two-layered microchannel was reduced by about 10% for both the parallel and counter-flow arrangement when compared with the single-layered microchannel. These results show that reduced pumping power can be achieved without increasing the total volume of the two-layered microchannel.

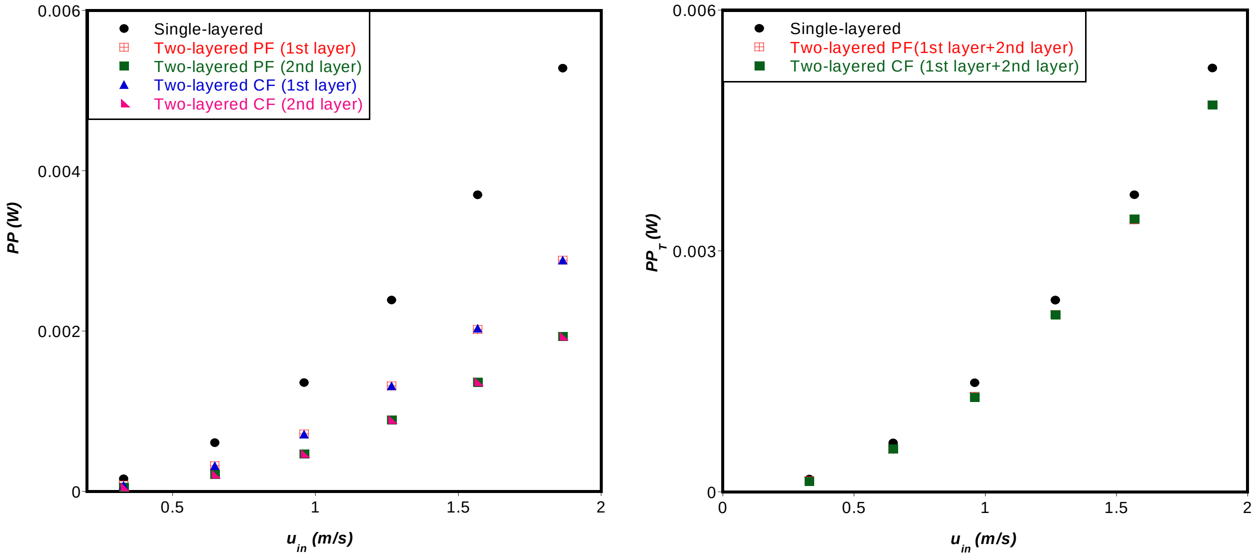


a) b)

Fig. 4 – Comparison between the pumping powers in the single and two-layered microchannels: a) each layer; b) total.

Figure 5 shows a comparison between the pumping power required for fluid flow through the single- and three-layered microchannels with the three different flow arrangements. In Fig. 5a, it was observed that the average pumping power required for the single-layered microchannels is 150% more than that required for each layer of the three-layered microchannels PF, CF1 and CF2. It was also shown that, for the three-layered PF, CF1 and CF2 the second layer required up to about 13% more pumping power than that of the first layer and about 15% more than the third layer. In Fig. 5b, the results show that when the total pumping power required for the three-layered microchannel was compared with the requirement for the single-microchannel, the three-layered PF, CF1, and CF2 requirements exceeded the requirement of the single-layered microchannel by an average of about 12%. These results show that, even though less pumping power was required in the two-layered microchannel, when the layers were increased to three with the same total volume, the total pumping power requirement for the same inlet fluid velocity range increased.

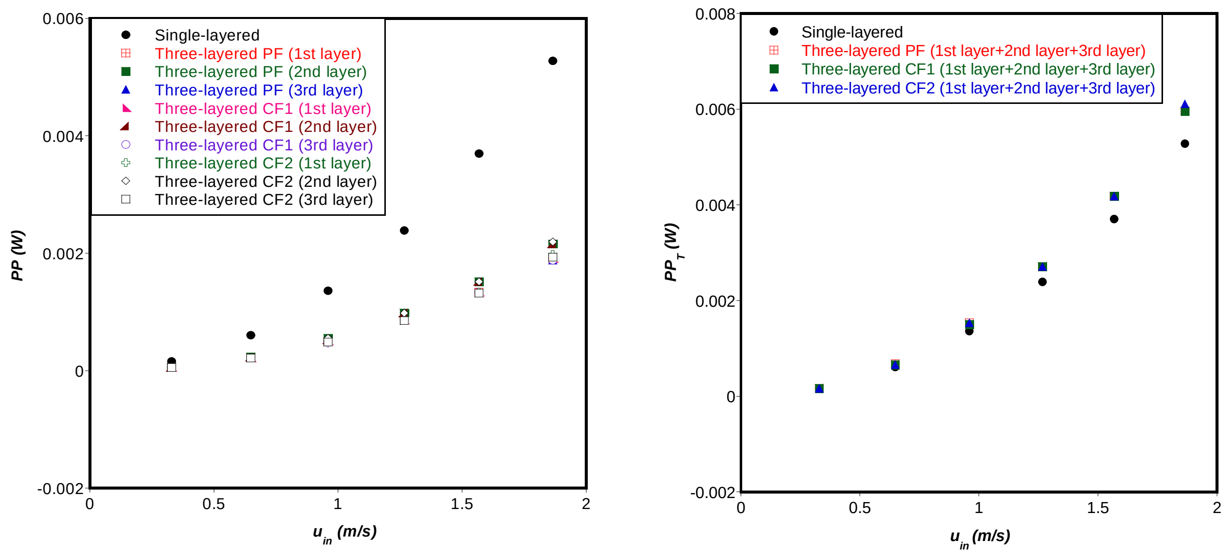


a) b)

Fig. 5 – Comparison between the pumping powers in the single and three-layered microchannels: a) each layer; b) total.

## 4. CONCLUSION

This paper presented three-dimensional numerical studies that investigated the heat transfer and fluid flow within different multi-layered microchannel heat sinks with different flow arrangements for a fixed total volume. Results from the multi-layered design were compared with those from single-layered microchannels with the same total volume and axial length. When results of pumping power requirement within the microchannels were compared, the two-layered microchannel with the different flow arrangements gave the least pumping power requirement for the range of fluid inlet velocity considered in this study.

## REFERENCES

1. X. WEI, Y. JOSHI, M.K. PATTERSON, *Experimental and numerical study of stacked micro-channel heat sink for liquid cooling of microelectronic devices*, Journal of Heat Transfer, **129**, pp. 1432–1444, 2007.
2. M.K. PATTERSON, X. WEI, Y. JOSHI, R. PRASHER, *Numerical study of conjugate heat transfer in stacked micro-channels*, Inter Society Conference on Thermal Phenomena, 2004, pp. 372–380.
3. K. JEEVAN, I.A. AZID, K.N. SEETHARAMU, *Optimization of double layer counter flow (DLCF) micro-channel heat sink used for cooling chips directly*, Electronics Packaging Technology Conference, 2004, pp. 553–558.
4. S.H. CHONG, K.T. OOI, T.N. WONG, *Optimization of single and double layer counter flow micro-channel heat sinks*, Applied Thermal Engineering, **22**, pp. 1569–1585, 2002.
5. O.O. ADEWUMI, T. BELLO-OCHENDE, J.P. MEYER, *Constructal design of combined microchannel and micro pin fins for electronic cooling*, International Journal of Heat and Mass Transfer, **66**, pp. 315–323, 2013.